

# Cytotoxicity of Zirconium Oxide Nanoparticles on Diabetic Rabbit Tooth Gum Cells

Parvaneh Naserzadeh<sup>1</sup>, Fatemeh Ghanbary<sup>2</sup>, Seyed Arash Javad Mossavi<sup>3</sup>, Masoud Akhshik<sup>4,5</sup> and Behnaz Ashtari<sup>6,7\*</sup>

<sup>1</sup>Endocrine Research Center, Institute of Endocrinology and Metabolism, Iran University of Medical Sciences, Tehran, Iran

<sup>2</sup>Department of Chemistry, Mahabad Branch, Mahabad, Iran

<sup>3</sup>Shahid Beheshti University of Medical Sciences. Tehran, Iran

<sup>4</sup>Centre for Bio composites and Biomaterials Processing. University of Toronto, Canada

<sup>5</sup>EPICentre, University of Windsor, Canada

<sup>6</sup>Radiation Biology Research Center, Iran University of Medical Sciences, Tehran, Iran

<sup>7</sup>Department of Medical Nanotechnology, Faculty of advanced technologies in medicine, Iran, University of Medical Sciences. Tehran, Iran

**Submission:** January 8, 2024; **Published:** February 2, 2024

**\*Corresponding author:** Behnaz Ashtari, Department of Medical Nanotechnology, Faculty of advanced technologies in medicine, Iran, University of Medical Sciences. Tehran, Iran, Emails: ashtaribeh@gmail.com

## Abstract

The cytotoxicity mechanism of zirconium oxide nanoparticles (ZrO<sub>2</sub>-NPs) has not been clarified to date. Nevertheless, generation of reactive oxygen species (ROS) by ZrO<sub>2</sub>-NPs has been considered as an important mechanism in some in vivo studies. The present study was conducted to identify the potential effects of ZrO<sub>2</sub>-NPs on diabetic rabbit tooth gum cells as well as the mechanisms of their cytotoxicity. ZrO<sub>2</sub>-NPs were characterized using scanning electron microscopy (SEM) and dynamic light scattering (DLS). Cell viability, ROS level, lipid peroxidation (MDA), mitochondrial membrane potential (MMP), glutathione count (GSH/GSSG), lysosome damage and apoptosis/ necrosis were evaluated. Biodistribution studies were conducted on tooth gum, liver, kidney, heart, and brain tissues in the diabetic rabbit using the inductively coupled plasma optical emission spectrometry (ICP/OES). ZrO<sub>2</sub>-NPs increased ROS, MMP collapse and MDA. In contrast, GSH/GSSG and apoptosis/ necrosis were found to be changed. The ZrO<sub>2</sub>-NPs accumulated significantly more on diabetic rabbit tooth gum tissues compared with other organs (P < 0.05). The study provided evidence that ZrO<sub>2</sub>-NPs cannot be considered completely biocompatible in the gum cell tissues of the diabetic rabbit. Before these nanoparticles can be used for human dental applications, further investigations on a wide range of cell death signaling should be performed.

**Keywords:** Cytotoxicity; Diabetic Rabbit; Reactive oxygen species; Tooth gum; Zirconium oxide nanoparticles

**Abbreviations:** ROS: Reactive Oxygen Species; DLS: Dynamic Light Scattering; MMP: Mitochondrial Membrane Potential; ICP/OES: Inductively Coupled Plasma/Optical Emission Spectrometry; DM: Diabetes Mellitus; BSA: Bovine Serum Albumin; FBS: Fetal Bovine Serum; IDF: International Diabetes Federation; SEM: Scanning Electron Microscopy; PB: Peripheral Blood; RBC: Red Blood Cell; HB: Hemoglobin; HCT: Hematocrit; MCHC: Mean Corpuscular Hemoglobin Concentration; MCH: Mean Corpuscular Hemoglobin, PDW: Platelet Distribution Width; PLT: Platelet Distribution width or Thrombocyte count; MPV: Mean Platelet Volume; WBC: White Blood Cell; SSC/FSC: Side Scattering/ Forward Scattering; MMP: Mitochondrial Membrane Potential; LPO: Lipid Peroxidation; TBARS: Thio Barbituric Acid Reactive Substances; GSH: Glutathione Redox; BMV: Bone Marrow Volume; TBV: Trabecular Bone Volume Tissue; OS: osteocytes; OB: osteoblasts; MPT: Mitochondrial Permeability Transition

## Introduction

The use of nanomaterials has increased notably in medicine and other biomedical fields. Although nanomaterials blend with the environment (air, water, and soil), there are serious concerns about their impact on human health as well as

environmental pollution that results from the distribution of kiln dust (nanoparticles or microparticles) [1]. The concentration of pollutants increases because of the increasing use of metal nanomaterials [1]. Nanomaterials such as single- and multi-walled

carbon nanotubes, nanofibers, quantum dots and metal oxide nanoparticles have been reported to be cytotoxic to human cells, bacteria, and rodents [2]. For example, cobalt nanoparticles cause damage to the human skin, and causes diseases such as rhinitis, asthma, allergic dermatitis, and cardiomyopathy [3]. Silver nanoparticles possess the highest degree of human cytotoxicity and environmental toxicity. Zinc oxide (ZnO), titanium dioxide (TiO<sub>2</sub>) and aluminum trioxide (Al<sub>2</sub>O<sub>3</sub>) nanoparticles adversely affect cell proliferation and viability in human lung epithelial cells [4]. Over the past decade, zirconium oxide nanoparticles (ZrO<sub>2</sub>-NPs), and TiO<sub>2</sub>-NPs have been extensively used in the semiconductor, thermoelectric, electro-optical, piezoelectric, painting, and dielectric materials industries. These nanoparticles are also incorporated into sunscreens, cosmetics, deodorants, and topical ointments. More recently, ZrO<sub>2</sub>-NPs have been used in biomedicine as drug delivery systems in conjunction with near-infrared light irradiation for anti-cancer therapy [1], as well as for diagnostic purposes. They have also been used for environmental decontamination because of their unique physicochemical features [1-6].

Dental materials and implants are an efficient alternative to traditional prostheses or bridges to restore missing teeth [7]. For the effectiveness of osseointegration, and the long-time survival of dental implants, the direct connection and capability between the implant and bone, without the intervention of soft tissues after implantation is very important [8]. Any disturbance in this biological mechanism will have a detrimental effect on the treatment outcome [8]. Diabetes mellitus (DM) is one of the chronic diseases that damage dental implant and provided peri-implantitis and poor osseointegration [8]. The Studies show a direct correlation between diabetic patients and bacterial infection around the implant [9]. Therefore, for the effectiveness of osseointegration in diabetic patients, it is necessary to use new materials. Zirconium oxide nanoparticles are used considerably in the ceramics industry and as dental and optical coatings. Previous studies reported that the cytotoxicity of these nanoparticles is dependent on their size and shape [10-11]. Although the toxic effects of ZrO<sub>2</sub>-NPs have not completely been elucidated, in vitro and in vivo studies have identified that ZrO<sub>2</sub>-NPs generate free radicals that damage vital intracellular macromolecules such as proteins and lipids. The free radicals are also responsible for apoptosis of different cell types [12-13]. Recently, high-strength ZrO<sub>2</sub> dental implants have been introduced as an alternative for the well-established titanium implants because of their improved fracture resistance and excellent flexural strength. Although ZrO<sub>2</sub> implants are becoming increasingly popular in oral implantology, the effects of their application on osteogenesis induction of mesenchymal stem cells have not been thoroughly investigated. Some studies reported that ZrO<sub>2</sub> dental implant systems do not possess clinical longevity [14-18]. Zirconia implants that replace maxillary first premolars have been evaluated for their long-term survival [19]. The biocompatibility of ZrO<sub>2</sub>-NPs and white Portland

cement has been evaluated [20]. Investigation of the extent of extracellular matrix (ECM) mineralization around ZrO<sub>2</sub> dental implants after 2 and 4 weeks of surgical implantation indicated that a slightly higher degree of bone apposition was achieved compared to titanium implants [21]. Accordingly, the cytotoxicity of ZrO<sub>2</sub>-NPs was investigated in the present study.

## Material and Methods

### Materials

3-[4,5-dimethylthiazol-2-yl]-2,5-diphenyltetrazolium bromide (MTT), dimethyl sulfide (DMSO), 2',7'-dichlorofluorescein diacetate (DCFH-DA) probes, Rhodamine 123 (Rh 123), Malondialdehyde (MDA), Thiobarbituric acid (TBA), n-butanol, Tetramethoxypropane (TEP), O-Phthalaldehyde (OPA) probe, N-Ethylmaleimide (NEM) probe, Acridine orange (AO), Ethylene Diaminetetraacetic acid (EDTA) were purchased from the Millipore Sigma. Annexin V FITC Apop Dtec Kit I, BD, Franklin Lake, USA were purchased from Sigma Chemical Co. (St. Louis, MO). Bovine serum albumin (BSA), fetal bovine serum (FBS) was purchased from Nichirei Bioscience, Tokyo, Japan and used without further purification. Zirconium (IV) tert-butoxide was purchased from the Merck KGaA, Darmstadt, Germany. Tetracycline hydrochloride and xylocaine/epinephrine were purchased from Showa Yakuhin Kako Co., Ltd., Tokyo, Japan. Alloxan monohydrate was provided from Sigma Aldrich BVBA, Overijse, Belgium.

### Instruments

During the testing process Fourier-transform infrared spectroscopy, IRTracer-100, Shimadzu, Kyoyo, Japan; Scanning electron microscopy, ALS -2100, Pooraka, South Australia, Australia; Zetasizer Nano ZS system, Malvern PAN alytical Inc, Westborough, MA, USA; Incubator 37°C, Sensor CO<sub>2</sub> Sanyo, Japan MCO; Vapor bath stark eliwellewpc 800T, UKA; Refrigerated Centrifugation, Sanyo, Harrier 18/80, Japan; Floremetry, Shimadzu RF-500, Japan; digital scale Japan; Shaker ,REAX2000®Iran; ELISA reader ,In finite 200 M, Tecan, Basel Switzerland; Flowcytometry, BD Biosciences FACS Calibure TM flow cytometer, hematological auto-analyzer ,Orphee Mythic 22 hematology analyzer, Diamond Diagnostics, Holliston, MA USA were used.

### Preparation of ZrO<sub>2</sub>-NPs

Stearic acid (569 g, 2 mol) was melted in a beaker at 73°C. Zirconium (IV) tert-butoxide (383.7 g, 1 mol) was added to the melted stearic acid under magnetic stirring. The mixture was heated in an oven at 300-400°C for 60-70 min. Impurities derived from stearic acid were removed in the form of H<sub>2</sub>O, CO<sub>2</sub> and CO. The mixture was then calcined at 850-900°C for 5 hours. Thereafter, the mixture was cooled to produce ZrO<sub>2</sub>-NPs [22].

### Characterization of ZrO<sub>2</sub>-NPs

Fourier-transform infrared spectroscopy was used to analyze the synthesized NPs. Scanning electron microscopy (SEM) was

used to examine the morphology of the NPs. Size distribution of the NPs was determined using a Zetasizer Nano ZS system [22].

### Antibacterial activity of $\text{ZrO}_2$ -NPs

Antibacterial evaluation was conducted for both Gram-positive (*Staphylococcus aureus*; ATCC 11775; American Type Culture Collection, Manassas, VA, USA) and Gram-negative bacteria such as *Escherichia coli* bacteria (ATCC; 25923). Antibacterial activities were evaluated using the modified Kirby-Bauer disk diffusion procedure. Briefly, the cells cultures were seeded in a Muller-Hinton chamber at a temperature of  $35 \pm 2^\circ\text{C}$  in a rotary spinner. For microbial growth, 100  $\mu\text{g}$  of fresh bacterial culture was diluted to  $10^6$  colonies forming units (CFU)/mL on the agar plates using a sterile glass-rod propagator. Afterward 10 min, 8 mm wells were connected to the anchor plates for testing the antimicrobial activity of the nanomaterials. All wells were sealed with agar to block the permeability of  $\text{ZrO}_2$ -NPs from the bottom of the wells. Using a micropipette, 100  $\mu\text{L}$  (50  $\mu\text{g}$ ) of  $\text{ZrO}_2$ -NP suspension was delivered to each well. Inhibition zones, if any, were measured after incubation overnight at  $35^\circ\text{C} \pm 2^\circ\text{C}$ . Rhea pure solvent and the antibiotic tetracycline were used as negative and positive control, respectively [23].

### Animals

Male rabbits (250-300 g each, 6 months old) were purchased from the Pasteur Institute of Iran. The animals were housed under controlled temperature ( $20\text{-}12^\circ\text{C}$ ) and relative humidity (50-60 %), as well as a 12-h light/dark cycle; they had free access to tap water and standard food. Five animals were used for each group (control and treatments;  $n = 5$ ). The study protocol was approved by the Animal Research Ethics Committee (AREC) of Iran Medical University. Efforts were made to minimize the number of animal experiments. After decapitating the rabbits, their tooth gum tissues were rapidly dissected and completely rinsed with isotonic saline. Peripheral blood (PB) samples were collected from the animals for isolation of the cells for subsequent characterization.

### Diabetic model procedure

All rabbits received a single dose of alloxan monohydrate (100 mg/kg period time, 1 min) using an intravenous cannula. To reduce risk of nephrotoxicity from hyperuricemia, a 7 ml/kg body weight iv injection of 0.9% saline was given immediately after the injection of alloxan at the rate of 1 mL/min. According to previous studies, to relieve the pain and distress from alloxan injection, the injection was performed under anesthesia. (medetomidine 0.25 mg/kg IM /ketamine 25 mg/kg bolus). A subcutaneous injection of 5% glucose solution (5 ml) was performed. Based on previous studies, animals that showed blood glucose levels above 250 mg/dL were considered diabetic [24].

### Surgical procedure

Operations were performed under sterile conditions. Each diabetic rabbit was anesthetized by intracardiac injection of

sodium pentobarbital. Anesthesia was maintained by inhalation of halothane (1.5-2.0 vol %). The root of the nose was shaved and disinfected using 70% ethanol. Local anesthesia was implemented using 2% xylocaine/epinephrine. A mucosal flap was made to expose the tooth gum laterally. Dental holes were made at eye level and 7 mm lateral toward the midline into the tooth gum area, using a 1-mm diameter, 4-mm long slow-speed dental drill under sterile saline irrigation. The  $\text{ZrO}_2$ -NPs were inserted into the hole at a concentration of 0.003 g using a sterile spatula. Each hole was then filled with amalgam. Tetracycline hydrochloride paste was injected into the surgical site to prevent bacterial infection [25].

### Stereological examination

The total volume of tissues was calculated using the Cavalieri method. A grid was superimposed over the images using stereological software. The volume was estimated using the formula [26]

$$V = \sum P x a / p x t$$

where “ $\Sigma P$ ” is the total points hitting the thrombus section, “ $a/p$ ” is the zone related to any point, and “ $t$ ” is the distance between the sampled sections. The numerical density of cells was determined using the optical dissector method. The position of the microscopic fields was selected by systematic uniform random sampling, with a moving stage in equal distances in x- and y-directions. A disinterested counting plate with inclusion and exclusion borders was superimposed on the images. A mikrokator was then attached to the stage of the microscope to measure the z-axis. The numerical densities (NV) were estimated using the formula:

$$Nv = \left[ \frac{\Sigma Q^-}{\Sigma P \times \frac{a}{f} \times h} \times \frac{t}{BA} \right]$$

where “ $\Sigma Q$ ” is the number of the cells coming into focus and counted, “ $\Sigma P$ ” is the total number of the counting frames in all fields,  $a/f$  is the area per frame, “ $h$ ” is defined as the height of the dissector, “ $t$ ” represents the real section thickness measured using the mikrokator when  $Q^-$  was counted, and  $BA$  represents the block advance of the microtome [27].

### Experimental design

The diabetic rabbits were randomly divided into two main groups. Group 1, health (0 day: before exposure) and group 2, experimental (0 day: before exposure) and six subgroups (1, 15 and 30 days, after exposure  $\text{ZrO}_2$ -NPs). In a pilot study, the NPs were prepared in different weight concentrations. After optimization of the isolated tooth gum cells on  $\text{ZrO}_2$ -NPs, experiments were subsequently conducted using 0.003 g of  $\text{ZrO}_2$ -NPs in normal saline. The  $\text{ZrO}_2$ -NPs were inserted in each diabetic rabbit's incisor tooth. The cells were isolated based on the experimental design.

### Nanoparticle distribution

Tooth gum tissues were analyzed by elemental analysis to determine the Zr content in the  $\text{ZrO}_2$ -NPs using a 10 mg L-1

standard stock solution (Agilent Technologies, Les Ulis, France). The samples were digested in ultrapure nitric acid overnight. Then, 0-3 mL of H<sub>2</sub>O<sub>2</sub> (30% (v/v)) was added to the solution and heated at 25 °C until the samples were completely digested. The remaining solutions were diluted by 3 mL nitric acid. The detection limit of ZrO<sub>2</sub>-NPs was 0.1 µg/mL by coupled plasma – optical emission spectrometry (ICP/OES). Data were expressed as ng/g of fresh tissue [28].

### Hematological analysis

Each diabetic rabbit was anesthetized through inhalation of 5% isoflurane. A blood sample (about 2 mL) was taken and placed into 2 polypropylene tubes. All blood samples were treated with EDTA to prevent coagulation. Serum was generated after the samples were centrifuged at 3,000rpm for 10 min. A hematological auto-analyzer was used to identify various hematological parameters such as red blood cell (RBC), Hemoglobin (HB), Hematocrit (HCT), corpuscular volume (MCV), mean corpuscular hemoglobin concentration (MCHC), mean corpuscular hemoglobin (MCH), platelet distribution width percent (PDW%), platelet distribution width or thrombocyte count (PLTs%), mean platelet volume (MPV), white blood cell (WBC) distribution width, lymphocytes (%), neutrophils (%), monocytes (%).

### Cellular toxicity assay

#### Fibroblast isolation

The diabetic rabbits' tissues were extracted after 1 month. Under local anesthetic, a small section of the gingiva (2×1×1mm) was removed using a scalpel. The tissues were immediately rinsed with boric acid for prevention of fungal infection. The gingiva tissues were placed in Dulbecco's Modified Eagle Medium (DMEM) that was supplemented with 10% FBS and penicillin 100 IU/mL, streptomycin 100 µg/mL and amphotericin B 100 µg/mL. The specimens were then rinsed with sterile PBS (PH ~7.4) and transferred to a petri dish containing DMEM, where it was mechanically minced. The tissue suspension and fibroblast cells were centrifuged (200 g for 5 min). The re-suspended pellet was placed in a plastic bottle containing the culture medium. The cells were incubated at 37°C in humidified air containing 5% CO<sub>2</sub>. The medium was renewed every 2 days [29].

#### Cell viability

Cells (~1×10<sup>6</sup> cells) isolated were subjected to flow cytometry cell sorting. The crude cells were dissolved in 0.5 mL PBS. One hundred microliter of aliquots was redistributed to the BD flow cytometry tube. Results of the side scattering/forward scattering (SSC/FSC) were analyzed for at least ~10,000 counts per sample in the flow cytometer [26]. Cell viability was evaluated by MTT staining. The cell viability (1×10<sup>4</sup> cells) test was based on the reduction of tetrazolium salt by intracellular dehydrogenases of

vital cells to purple formazan. The latter was dissolved in dimethyl sulfoxide for measuring the absorbance at 570 nm using a plate reader. The experiment was conducted in triplicate [30].

### Reactive Oxygen species production

The cells (1×10<sup>6</sup> cells) were fed with both culture medium and ZrO<sub>2</sub>-NPs. The Reactive Oxygen species production (ROS) level was evaluated before and after the treatment. After the treatment, cells were washed with PBS as previously described. Ten microliter of DCFH-DA was used to measure intracellular ROS after interaction with fluorescent DCFH-DA. Fluorescence was measured using a spectrophotometer at  $\lambda_{\text{excitation}}/\lambda_{\text{emission}} = 490/535$  nm [31].

### Mitochondrial membrane potential (MMP)

The cells (1×10<sup>6</sup> cells) were treated with both the culture medium and ZrO<sub>2</sub>-NPs before and after culture. Cell aliquots were incubated with Rh 123, a lipophilic, cationic fluorescent dye, at room temperature for 20 min in the dark with diluted PBS. The fluorescence intensity of the dye is quenched when it accumulates in the mitochondria. Dye uptake was measured with a spectrophotometer. Fluorescence was measured at  $\lambda_{\text{excitation}}/\lambda_{\text{emission}} = 490/535$  nm. The uptake capacity of the cells was also measured [32].

### Lipid peroxidation

the lipid peroxidation (LPO) was assayed by the determination of the amount of thiobarbituric acid reactive substances (TBARS) formed during the decomposition of lipid hydroperoxides on isolated cells (1×10<sup>6</sup> cells/well) by following the absorbance at 532 nm in a spectrophotometer analyzer by determining the MDA level following the manufacturer's instructions. Each test/group was examined with three replicates for each sample [33].

### Glutathione redox state

On isolated cells, (1×10<sup>6</sup> cells/well), glutathione redox (GSH) by OPA probe and glutathione oxidase (GSSG) by NEM probe are the most important scavengers of ROS that can be utilized as a biomarker of the redox balance. Each sample was measured in quartz cuvettes using a fluorimeter set at  $\lambda_{\text{excitation}}/\lambda_{\text{emission}} = 350/420$  nm wavelengths. Each test/group was examined with three replicates for each sample [33].

### Lysosome membrane integrity

Cell suspension (1×10<sup>6</sup> cells/well) was stained with AO (5 µM), an indicator of lysosome membrane permeabilization. The cells were separated from the incubation plate by centrifugation at 1000 rpm for 1 min. The cell pellet was re-suspended in 2 mL of fresh culture medium and rinsed twice to remove the fluorescent dye. AO redistribution in the cell suspension was



measured colorimetrically using a spectrophotometer at  $\lambda_{\text{excitation}}/\lambda_{\text{emission}} = 490/535$  nm. Lysosome membrane damage is defined as the difference in the redistribution of AO from lysosomes into the cytosol between the treated and control cells [34].

### Apoptosis and Necrosis assay

After the treatment, the cells ( $1 \times 10^6$  cells/well) were stained with 5 ml of Annexin V and 5 ml of PI at room temperature for 20 min. The cells were diluted in the binding buffer (400  $\mu$ l) and analyzed with flow cytometry. The fluorescence signals of Annexin V and PI were measured by flow cytometry on the FL1 and FL3 channels. Supplied with the softwaring 1.2.5 and each determination is based on the mean fluorescence intensity of 10,000 counts and following the manufacturer's instructions.

### Statistical analysis

All data sets were normally distributed and homoscedastic. Hence, the data were analyzed using one-way and two-way analysis of variance followed by post-hoc Tukey and Bonferroni tests, respectively. Results were presented as mean  $\pm$  standard deviation ( $n = 5$ ), with statistical significance pre-set at  $\alpha = 0.05$ .

### Results

#### ZrO<sub>2</sub>-NP characterization

The morphology of the prepared ZrO<sub>2</sub>-NPs is shown in Figure 1A. Size distribution of the NPs, as measured by their hydrodynamic diameter (dh) is presented in Figure 1B.

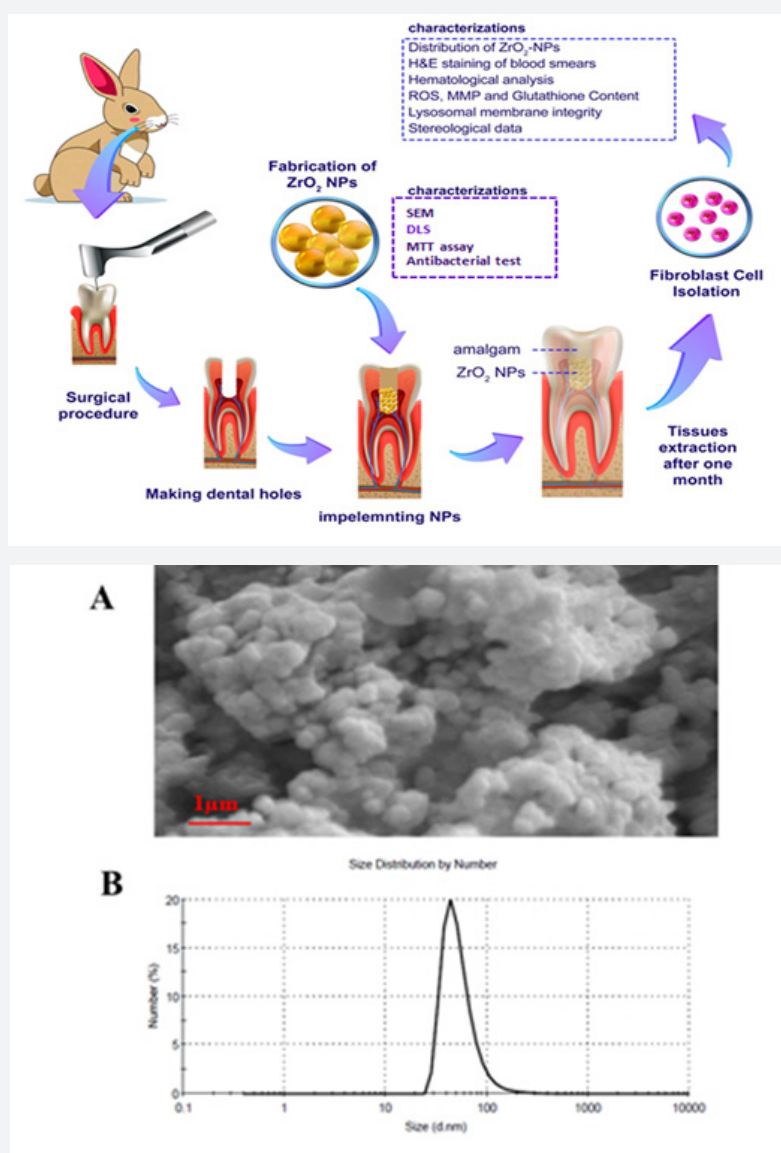


Figure 1: : Characterization of ZrO<sub>2</sub>-NPs by SEM (A), size distribution of the hydrodynamic diameter of the ZrO<sub>2</sub>-NPs (B).

### Distribution of ZrO<sub>2</sub>-NPs

Distribution of ZrO<sub>2</sub>-NPs in the brain, heart, lungs, kidneys, and liver at days 0 (before exposure of NPs) 1, 15 and 30 (after exposure to the NPs) is shown in Table 1. In ZrO<sub>2</sub>-NP treatment (CD) group, the NPs were accumulated predominantly in the

tooth gum after 15 and 30 days. Accumulation of ZrO<sub>2</sub>-NPs was barely detectable in the brain, heart, kidneys, lungs, and liver. Accumulation of the ZrO<sub>2</sub>-NPs in the tooth gum tissues was  $1.1 \pm 0.11$  µg/g after 1 days,  $2 \pm 0.1$  µg/g after 15 days and  $1.4 \pm 0.1$  µg/g after 30 days (\*P < 0.05) and 0 (before exposure of NPs) in all of tissue had not any accumulation of ZrO<sub>2</sub>-NP.

**Table 1:** Distribution of ZrO<sub>2</sub>-NPs in the brain, heart, lungs, kidneys, and liver of diabetic rabbits at 0 (before exposure time), 1, 15 and 30 days (after exposure time). Values are expressed as means  $\pm$  SD (n = 5). ns: non-significant; \*P<0.05; compared to control cells before exposure.

ZrO <sub>2</sub> -NP content in different tissues				
Tissue	Concentration of ZrO <sub>2</sub> (µg/g)			
	Before	After		
	0 day	1 day	15 days	30 days
Tooth gum	<0.1	$1.1 \pm 0.1^*$	$1.2 \pm 0.1^*$	$1.4 \pm 0.1^*$
Brain	<0.1	<0.1 <sup>ns</sup>	<0.1 <sup>ns</sup>	<0.1 <sup>ns</sup>
Heart	<0.1	<0.1 <sup>ns</sup>	<0.1 <sup>ns</sup>	<0.1 <sup>ns</sup>
Lungs	<0.1	<0.1 <sup>ns</sup>	<0.1 <sup>ns</sup>	<0.1 <sup>ns</sup>
Kidneys	<0.1	<0.1 <sup>ns</sup>	<0.1 <sup>ns</sup>	<0.1 <sup>ns</sup>

### Antimicrobial properties

The ZrO<sub>2</sub>-NPs did not exhibit antibacterial activity against Gram-positive nor Gram-negative bacteria (Figure 2A). As shown

in Figure 2B, no inhibition zones were identified when disks containing ZrO<sub>2</sub>-NPs were in placed in contact with *S. aureus* or *E. coli*.

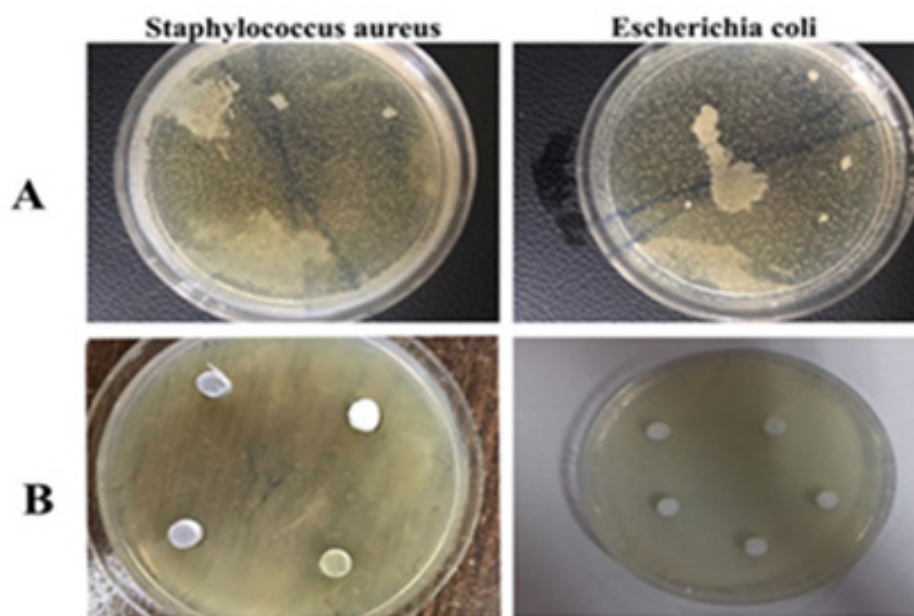


**Figure 2:** Agar diffusion methods: disk-diffusion of microbial extracts using *Staphylococcus aureus* and *Escherichia coli* as test microorganisms (A). Antibigram test in agar culture of *S. aureus* and *E. coli* of ZrO<sub>2</sub>-NPs.

### Stereological examination

Images from the control health group (CH) and ZrO<sub>2</sub>-NP treatment group (CD) (B) are shown in Figure 3A volume of epithelium (V. E mm) and connective tissue (V. CT), and number

of neutrophils (N.N) in tooth gum tissue. B. Estimation of the total volume of bone (TV), Figure 3B bone marrow volume (BMV), trabecular bone volume tissue (TBV), osteocytes (OS) and osteoblasts (OB) in the tooth gum tissue showed no significant differences between the CH and CD groups (Table 5A, B).

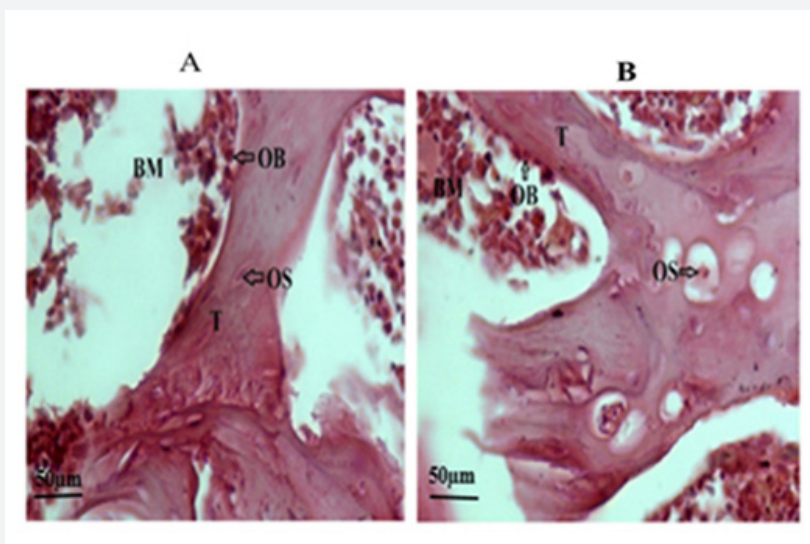


**Figure 3:** Stereological examination of tissue bone marrow volume (BM), trabecular bone volume tissue (T), osteocyte (OS) and osteoblast (OB). There is no significant difference between the control health(A) and ZrO<sub>2</sub>-NP treatment (CD) (B) groups. The density of tissue is equal to 50 µm.

**Table 2:** Difference in hematological parameters between control health (CH) and ZrO<sub>2</sub>-NP treatment (CD) at 0 (before exposure time), 1, 15 and 30 days (after exposure time). Values are expressed as means  $\pm$  SD (n = 5). ns: non-significant; \*P<0.05; \*\*P<0.01; compared to control cells before exposure.

White blood cells (count; cells 10 <sup>6</sup> )								
Parameter	Control				Experimental			
	Before	After			Before	After		
	0 day	1 day	15 days	30 days	0 day	1 day	15 days	30 days
WBC	5.44 $\pm$ 0.05	5.62 $\pm$ 0.08 <sup>ns</sup>	5.72 $\pm$ 0.07 <sup>ns</sup>	5.75 $\pm$ 0.04 <sup>ns</sup>	5.55 $\pm$ 0.11 <sup>ns</sup>	6.50 $\pm$ 0.43*	6.62 $\pm$ 0.41*	6.69 $\pm$ 0.36*
Lymphocytes	12.0 $\pm$ 1.0	12.4 $\pm$ 1.0 <sup>ns</sup>	17.3 $\pm$ 1.15 <sup>ns</sup>	17.0 $\pm$ 1.0 <sup>ns</sup>	12.22 $\pm$ 3 <sup>ns</sup>	15.7 $\pm$ 3.1 <sup>ns</sup>	19.7 $\pm$ 2.3*	24.0 $\pm$ 4.0**
Monocytes	3.0 $\pm$ 0.41	3.33 $\pm$ 0.57 <sup>ns</sup>	3.33 $\pm$ 0.57 <sup>ns</sup>	3.66 $\pm$ 1.10 <sup>ns</sup>	3.20 $\pm$ 0.57 <sup>ns</sup>	3.33 $\pm$ 0.57 <sup>ns</sup>	3.99 $\pm$ 0.01*	4.66 $\pm$ 0.57*
Neutrophils	46.22 $\pm$ 1	46.7 $\pm$ 1.5 <sup>ns</sup>	44.0 $\pm$ 1.0 <sup>ns</sup>	45.0 $\pm$ 1.0 <sup>ns</sup>	45.02 $\pm$ 2.0 <sup>ns</sup>	46.0 $\pm$ 1.0 <sup>ns</sup>	64.0 $\pm$ 1.0**	66.0 $\pm$ 1.0**

**Table 3:** Hematological evaluation of various parameters on control health (CH) and ZrO<sub>2</sub>-NP treatment (CD) at 0 (before exposure time), 1, 15 and 30 days (after exposure time). Values are expressed as means  $\pm$  SD (n = 5). ns: non-significant; \*P<0.05; \*\*P<0.01; \*\*\*P<0.001; compared to control cells before exposure.

Hematological evaluation of various parameters								
Parameter	Control				Experimental			
	Before	After			Before	After		
	0 day	1 day	15 days	30 days	0 day	1 day	15 days	30 days
RBC	4.40 $\pm$ 0.06	4.45 $\pm$ 0.03 <sup>ns</sup>	4.53 $\pm$ 0.02 <sup>ns</sup>	4.54 $\pm$ 0.02 <sup>ns</sup>	4.22 $\pm$ 0.02 <sup>ns</sup>	4.103 $\pm$ 0.005 <sup>ns</sup>	4.14 $\pm$ 0.05 <sup>ns</sup>	4.19 $\pm$ 0.10 <sup>ns</sup>
HB	14.12 $\pm$ 0.10	14.26 $\pm$ 0.15 <sup>ns</sup>	14.12 $\pm$ 0.12 <sup>ns</sup>	14.25 $\pm$ 0.02 <sup>ns</sup>	14.23 $\pm$ 0.1 <sup>ns</sup>	14.44 $\pm$ 0.11 <sup>ns</sup>	14.53 $\pm$ 0.10 <sup>ns</sup>	14.64 $\pm$ 0.09 <sup>ns</sup>

<b>MCH</b>	25.33±0.05	25.42±0.03 <sup>ns</sup>	25.45±0.02 <sup>ns</sup>	25.54±0.01 <sup>ns</sup>	25.1±0.1*	27.00±0.51*	27.15±0.53*	27.45±0.83*
<b>MCHC</b>	30.11±0.07	30.12±0.02 <sup>ns</sup>	30.13±0.01 <sup>ns</sup>	30.14±0.02 <sup>ns</sup>	35.14±0.33**	37.14±0.71**	37.41±0.29***	37.53±0.21***
<b>PLTs</b>	150±1.0	154±1.5 <sup>ns</sup>	155±1.7 <sup>ns</sup>	156±1.5 <sup>ns</sup>	203±12**	219±16.5***	222±16.9***	227±16.1***
<b>HCT</b>	39.07±0.1	39.7±0.1 <sup>ns</sup>	39.53±0.6 <sup>ns</sup>	40.4±0.3 <sup>ns</sup>	39.88±0.5 <sup>ns</sup>	39.92±0.3 <sup>ns</sup>	40.88±1.0*	42.81±3.63*
<b>MCV</b>	88.33±0.10	88.70±0.17 <sup>ns</sup>	88.67±0.01 <sup>ns</sup>	88.73±0.02 <sup>ns</sup>	88.80±0.40 <sup>ns</sup>	88.84±0.33 <sup>ns</sup>	88.86±0.43 <sup>ns</sup>	88.97±0.38 <sup>ns</sup>
<b>PDW %</b>	11.32±0.10	11.66±0.15 <sup>ns</sup>	11.00±1.00 <sup>ns</sup>	11.55±0.01 <sup>ns</sup>	12.33±0.21 <sup>ns</sup>	12.44±0.19 <sup>ns</sup>	12.62±0.13 <sup>ns</sup>	12.73±0.21 <sup>ns</sup>
<b>MPV</b>	8.09±0.06	8.11±0.02 <sup>ns</sup>	8.24±0.03 <sup>ns</sup>	8.33±0.02 <sup>ns</sup>	8.06±0.01 <sup>ns</sup>	8.46±0.08 <sup>ns</sup>	8.54±0.10 <sup>ns</sup>	8.61±0.11 <sup>ns</sup>

**Table 4:** Ratio of Intracellular GSH and extracellular GSSG concentrations on control health (CH) and ZrO<sub>2</sub>-NP treatment (CD) cells (1×10<sup>4</sup> cells/well) at 0 (before exposure time), 1, 15 and 30 days (after exposure time). Values are expressed as means ± SD (n = 5). ns: non-significant; \*P<0.05; \*\*P<0.01; compared to control cells before exposure.

Glutathione content (µg/mg protein)								
Parameter	Control				Experimental			
	Before	After			Before	After		
	0 day	1 day	15 days	30 days	0 day	1 day	15 days	30 days
<b>GSH</b>	286±0.008	286±0.008 <sup>ns</sup>	279±0.006 <sup>ns</sup>	277±0.007 <sup>ns</sup>	224±0.07*	232±0.005*	246±0.004*	213±0.004*
<b>GSSG</b>	360±0.020	360±0.020 <sup>ns</sup>	365±0.014 <sup>ns</sup>	363±0.021 <sup>ns</sup>	557±0.01**	561±0.001**	594±0.011**	614±0.005**
<b>GSSG/GSH</b>	1.3±0.020	1.3±0.020 <sup>ns</sup>	1.3±0.014 <sup>ns</sup>	1.3±0.021 <sup>ns</sup>	2.4±0.01*	2.4±0.001*	2.4±0.011*	2.9±0.005*

**Table 5:** Stereological study. A. Estimation of the V. E, V. CT, N.N in tooth gum tissue. B. Estimation of the total volume of TV, BMV, TBV, OS and OB in jawbone tissue on control health (CH) and ZrO<sub>2</sub>-NP treatment (CD). Values are expressed as means ± SD (n = 5). \*P<0.05; \*\*P<0.01; \*\*\*P<0.001; compared to control health before exposure.

Stereological Examinations (µm)								
Groups	A: Tooth gum			B: Jawbone				
	N. N	V. CT	V. E (mm)	TV (mm <sup>3</sup> )	BMV (mm <sup>3</sup> )	TBV (mm <sup>3</sup> )	O <sub>s</sub>	OB
<b>CH</b>	37	35.9	52.6	429.5	25.5	115.8	32	27
<b>CD</b>	132***	58.1**	91.1**	417.3*	24.1*	108.6*	31*	28*

## Hemotoxicity

Hematoxylin and eosin-stained blood smears of the control health group (CH) (A) and ZrO<sub>2</sub>-NP treatment group (CD) are shown in Figure 4. At 1 day's post-treatment, hemotoxicity was absent from the peripheral blood samples obtained from diabetic rabbits treated with ZrO<sub>2</sub>-NPs compared control health group (before time).

## Hematological analysis

Increase of white blood cell (WBC) count in ZrO<sub>2</sub>-NP treatment groups after 1, 15 and 30 day (\*P<0.05), The percentage of lymphocytes population in 15 (\*P<0.05) and 30 days (\*\*P<0.01), The percentage of monocytes population in 15 (\*P<0.05) and 30 day (\*P<0.05), The percentage of neutrophils population in 15 (\*\*P<0.01) and 30 days (\*\*P<0.01). All of group were not significant compared with control health (CH, 0day) group all of time (Table 2). counts of RBC count in the experimental group after administration of the ZrO<sub>2</sub>-NP was not significant in all of

time compared with control health (CH, 0 day) (Table 3). HB did not significantly change after treatment with ZrO<sub>2</sub>-NPs in the experimental and health group after 1, 15 and 30 days compared with control health (CH, 0 day) (Table 3). MCH increased in 0, 1, 15 and 30 days after treatment of the ZrO<sub>2</sub>-NP in experimental group compared with control health (CH, 0 day) (Table 3). Significant induction of MCHC after exposure ZrO<sub>2</sub>-NPs in the experimental group in 0, 1 day (\*\*P<0.01), 15 and 30 day (\*\*\*P<0.001) compared with control health (CH, 0 day) and other groups were not significant change in factor (Table 3). PLTs was increased after ZrO<sub>2</sub>-NP administration in experiment groups after 0, 1, 15 and 30 days (\*\*P<0.01) compared with control health (CH, 0 day) and other groups were not significant change in factor (Table 3). HCT was increased after ZrO<sub>2</sub>-NP administration in experiment groups after 0, 1, 15 and 30 day (\*P<0.05) compared with control health (CH, 0 day) and other groups were not significant change in factor (Table 3). In MCV, PDW% and MPV were not any change on experimental groups after exposure ZrO<sub>2</sub>-NPs all of time (Table 3).



### Cell viability

The percentage of total cell viable (Q1) population were CH~ 94.3%, CH.1~ 92.88%, CH.15~ 98.56%, CH.30~ 90.64%, CD~ 89.78%, CD.1~ 78.86%, CD.15~ 72.35%, CD.30~ 59.37%. Changed garrulity (Q2) population were CH~ 1.41%, CH.1~ 0.48%, CH.15~ 0.1%, CH.30~ 4.90%, CD~ 0.99%, CD.1~ 0.97%, CD.15~ 0.23%, CD.30~ 11.06%. Changed morphology/granulity (Q3) population were CH~ 2.82%, CH.1~ 1.09%, CH.15~ 0.11%, CH.30~ 0.09%, CD~ 2.09%, CD.1~ 1.89%, CD.15~ 10.50%, CD.30~ 15.49%. Changed morphology (Q4) population were CH~ 1.62%, CH.1~ 5.64%, CH.15~ 1.23%, CH.30~ 4.37%, CD~ 7.13%, CD.1~ 18.28%, CD.15~ 16.90%, CD.30~ 13.97% (Figure 5A). cell viability as evaluated by MTT staining, was significantly reduced after 0, 1,15 days(\*\*P<0.01), 30(\*\*P<0.001) incubation of cells with ZrO<sub>2</sub>-NPs in experimental group compared with control

group (CH, 0 day) (Figure 5B).

### Reactive oxygen species and mitochondrial membrane potential

Application of ZrO<sub>2</sub>-NPs significantly elevated ROS generation in cells obtained from tooth gum tissue (Figure 6A); generation of ROS was concentration- and time-dependent. Administration of ZrO<sub>2</sub>-NPs in experimental group after 1,15 (\*P<0.05) and 30 days(\*\*P<0.01) compared with control group (CH, 0 day). Significantly reduced the mitochondrial membrane potential in tooth gum cells in a concentration- and time-dependent manner, as indicated by the increase in cellular uptake of Rh123 after exposure of ZrO<sub>2</sub>-NPs in experimental group on 15 and 30 days(\*\*P<0.001) compared with control group (CH, 0 day). (Figure 6B).

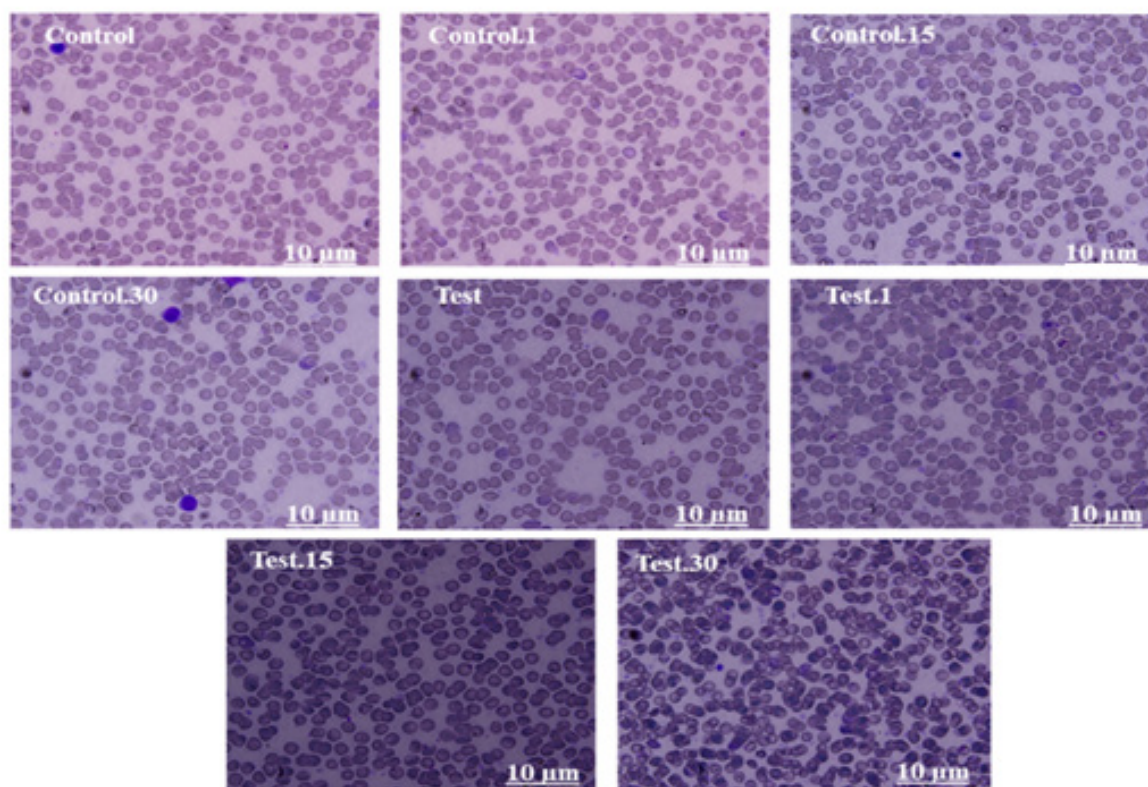


**Figure 4:** Hematoxylin and eosin staining. Photomicrographs of the collected blood on control health (CH) and ZrO<sub>2</sub>-NP treatment (CD) at 0 (before exposure time), 1, 15, 30 days (after exposure time). Magnification x100.

### Glutathione content

Significant decrease GSH levels in CD group (0 day) and administration of ZrO<sub>2</sub>-NPs in experimental group after 1,15 and 30 day (\*P<0.05) compared with control group (CH, 0 day). Cells

in CD group (0 day) and exposed to ZrO<sub>2</sub>-NPs in experimental groups and significantly increased on GSSG contents after 1,15 and 30 days (\*\*P<0.01) compared with control group (CH, 0 day) and finally GSSG/GSH was changing treatment groups (Table 4).

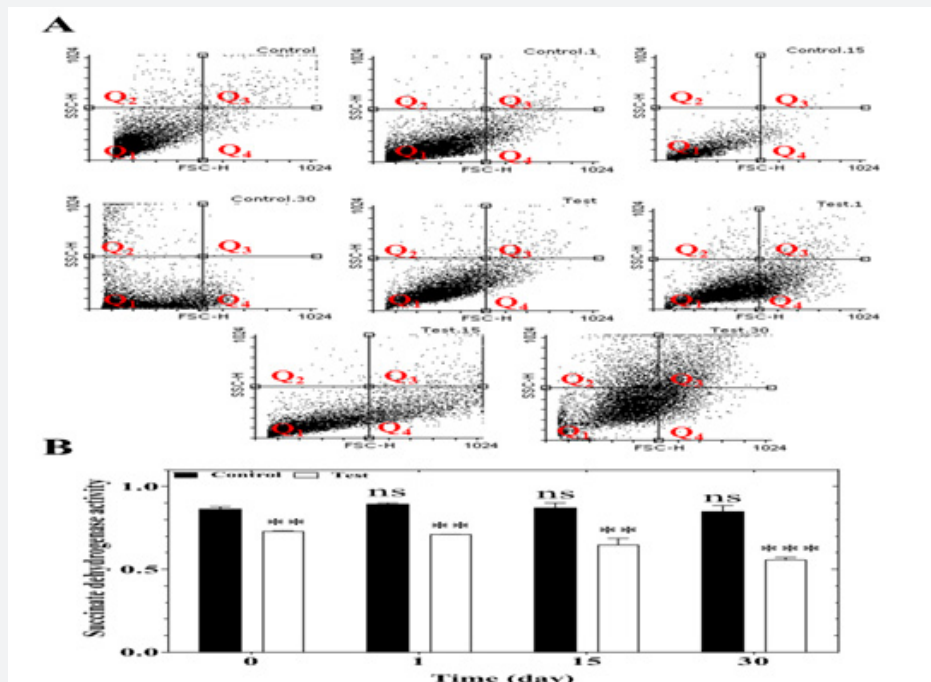


**Figure 5:** Flow cytometry of viable tooth gum cells (10,000 counts) (A) and cell viability assay (1×10<sup>4</sup> cells/well) (B) on control health (CH) and ZrO<sub>2</sub>-NP treatment (CD) at 0 (before exposure time), 1, 15, 30 days (after exposure time). Values are expressed as means ± standard deviations (n = 5). ns: non-significant; \*\*P<0.01; \*\*\*P<0.001; compared to control cells.

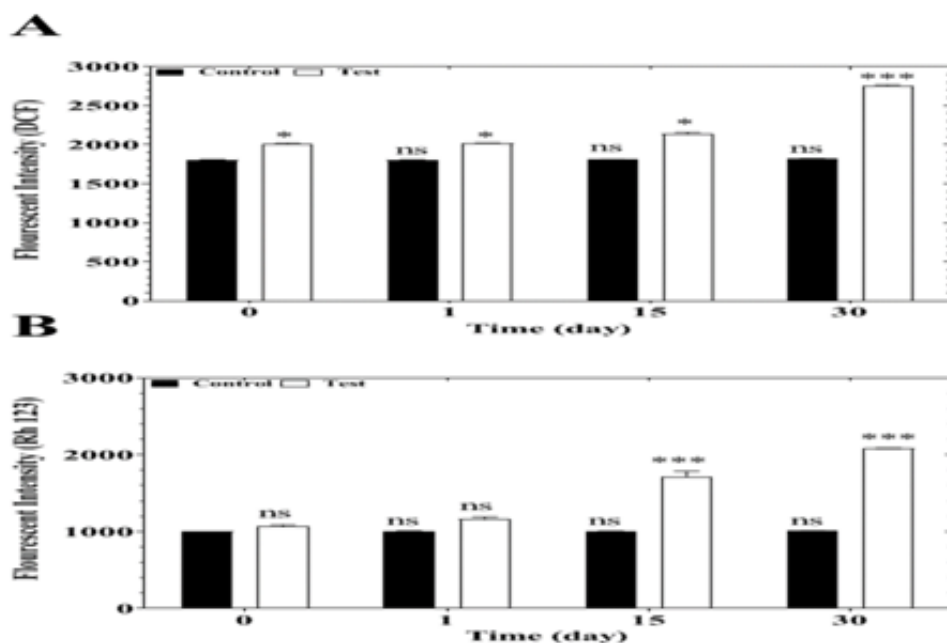


**Figure 6:** ROS formation was expressed as fluorescent intensity (1×10<sup>4</sup> cells/well) (A) and MMP was expressed as fluorescent intensity (1×10<sup>4</sup> cells/well) (B) on control health (CH) and ZrO<sub>2</sub>-NP treatment (CD) at 0 (before exposure time), 1, 15 and 30 days (after exposure time). Values represented as mean ± SD (n = 5). ns=no significant, \*P < 0.05 and \*\*\*P < 0.001 compared with control health (CH) group.

### Lipid peroxidation and lysosomal membrane integrity

Administration ZrO<sub>2</sub>-NPs in experimental groups caused a significant increase in the MDA levels in the tooth gum cells at day 1 (\*\*P < 0.01), 15 and 30 (\*\*P < 0.001). Thereafter, there was no significant difference in the MDA levels between health

groups before and 1,15, 30 days (Figure 7A). There were also significant increases in lysosomal membrane permeabilization in the experimental group before (\*P < 0.05) and after exposure to ZrO<sub>2</sub>-NPs for 11 (\*\*P < 0.01), 15 and 30 days1 (\*\*P < 0.001), as revealed by the increase in uptake of AO (Figure 7B).

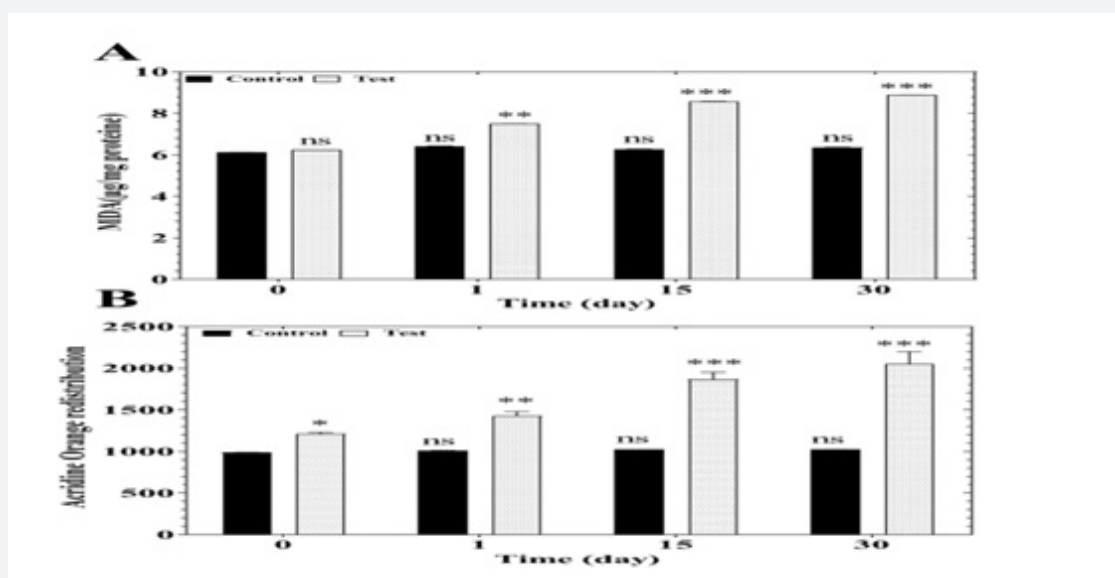


**Figure 7:** Thiobarbituric Acid Reactive Substances assay for quantification of MDA, the end-products of lipid peroxidation (1×10<sup>4</sup> cells/well) (A) on control health (CH) and ZrO<sub>2</sub>-NP treatment (CD) at 0 (before exposure time), 1, 15, 30 days (after exposure time). Lysosomal membrane integrity (1×10<sup>4</sup> cells/well) (B) shows that there is a significant difference between the integrity of lysosomal membranes on control health (CH) and ZrO<sub>2</sub>-NP treatment (CD) at 0 (before exposure time), 1, 15 and 30 days (after exposure time). Values represented as mean ± SD (n = 5). ns=no significant, \*P < 0.05; \*\*P < 0.01 and \*\*\*P < 0.001 compared with control health (CH) group.

### Apoptosis and Necrosis

The apoptosis was quantified by the externalization of PS (phosphatidylserine). PI stains the nuclear and, thus, it was used as an indicator of membrane integrity and finally apoptosis/necrosis assessed by annexin V/PI double staining at cell viable (Q1) population were CH~ 99.27%, CH.1~ 99.20%, CH.15~ 99.17%, CH.30~ 99.17%, CD~ 93.67%, CD.1~ 87.45%, CD.15~ 75.72%, CD.30~ 60.63%. necrosis (Q2) population were CH~ 0.56%, CH.1~ 0.13%, CH.15~ 0.16%, CH.30~ 0.07%, CD~ 5.70%, CD.1~ 0.37%, CD.15~ 10.29%, CD.30~ 28.75%. Early apoptotic (Q3) population were CH~ 0.6%, CH.1~ 0.24%, CH.15~ 0.30%, CH.30~ 0.42%, CD~ 0.51%, CD.1~ 3.60%, CD.15~ 11.14%, CD.30~ 8.01%. Late apoptotic (Q4) population were CH~ 0.09%, CH.1~ 0.43%, CH.15~ 0.37%, CH.30~ 0.34%, CD~ 0.08%, CD.1~ 8.58%, CD.15~ 2.72%, CD.30~ 2.43% (Figure 8).

### Discussion

Diabetes mellitus is known as an endocrine disorder and the number of sufferers has been increasing in recent years. According to the prediction of the International Diabetes Federation (IDF), the number of diabetics will increase to 578.4 million people

by 2030 and to 700 million people by 2045. In most cases, due to the lack of effective control, this disease causes significant complications [7]. The various complications include neurological disorders, narrowing of blood vessels, blindness in adulthood, end-stage renal disease, ischemia, peripheral vascular disease, microbial infections, and loss of dental implants [8]. A few studies have shown that despite high bone density in female diabetic patients compared to their male counterparts, the fracture rate in women is higher, which indicates a qualitative difference in bone [35]. In addition, in diabetic patients, osteoblastic activity is limited, and parathyroid hormones change calcium and phosphorus metabolism. As a result, collagen fiber formation is reduced, and bone cells may undergo apoptosis and prevent bone formation [36].

Zirconium oxide nanoparticles are used considerably in the ceramics industry and as dental and optical coatings. Previous studies reported that the cytotoxicity of these nanoparticles is dependent on their size and shape [13-14]. It has been speculated that ZrO<sub>2</sub>-NPs are potentially cytotoxic because of their potential to induce cellular oxidative stresses. The latter, in turn, results in increased ROS production, reduced GSH levels, and augmented

lipid peroxidation. The lack of evidence supporting these hypotheses in antecedent studies prompted us to investigate the

in vitro and in vivo cytotoxicity of  $\text{ZrO}_2$ -NPs on diabetic rabbit tooth gum cells.

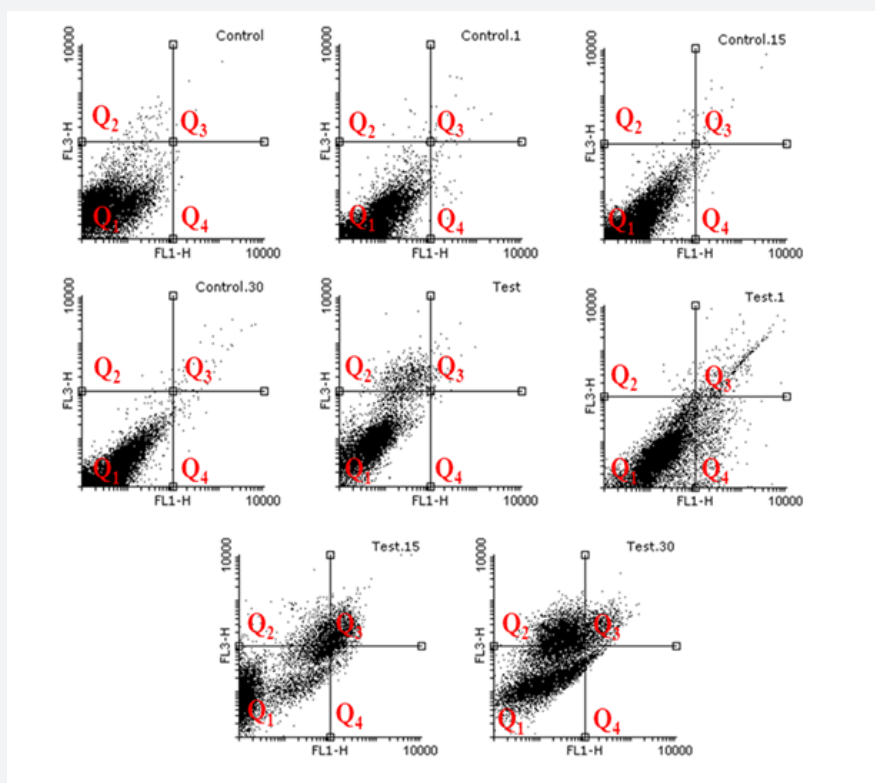


**Figure 8:** determination of apoptotic and necrotic (annexin V/PI) markers on cells ( $1 \times 10^4$  cells/well) by flowcytometry on control health (CH) and  $\text{ZrO}_2$ -NP treatment (CD) at 0 (before exposure time), 1, 15 and 30 days (after exposure time).

Results obtained from the present study indicate that increased intracellular ROS after exposure to  $\text{ZrO}_2$ -NPs is responsible for the cytotoxicity of these NPs in vitro and in vivo. These results are in general agreement with previous reports in the literature. The generation of ROS is caused by electron ‘leakage’ of the mitochondrial respiratory chain, which can be evaluated by the production of dichlorofluorescein, the highly fluorescent oxidized derivative of dichloro-fluorescein diacetate. These ROS originate from superoxide production either from complex I or from ubiquinone/complex III, due to partial damage and/or inhibition of the respiratory chain complexes [33]. Several authors claimed that ROS generation stimulates pro-apoptotic cell signaling via cytochrome c release from mitochondria [32,33].

Although the effect of ROS on cellular damage has not been completely elucidated [33], some studies suggested that lipid peroxidation plays a crucial role in NP-induced cytotoxicity [36, 37]. This hypothesis was supported by the results obtained from the present study. Increased ROS generation results in oxidation of the thiol group of membrane proteins. This, in turn, induces opening of the mitochondrial permeability transition (MPT) pores, which precipitate mitochondrial dysfunction. The

latter is manifested by unlimited proton movement across the inner mitochondrial membrane as well as induction of MMP disruption and uncoupling of oxidative phosphorylation [38]. It has been proposed that cell membrane damage occurs via lipid peroxidation, which initiates a chain of reactions that further results in cellular degradation [39]. Several authors have reported that  $\text{ZrO}_2$ -NPs generate ROS and oxidative stress of occurs through induction of death intracellular signaling pathways [38,39]; ROS generation adversely affect DNA and transcription of proteins that are responsible for membrane integrity, subsequently resulting in the loss of membrane integrity [40-44]. Others suggested that  $\text{ZrO}_2$ -NPs induce apoptosis in T-helper lymphocytes at concentrations higher than 5 mM, through increasing the release of tumor necrosis factor-alpha [45].

Contrary to these reports, Damestani et al. reported that  $\text{ZrO}_2$ -NPs are biocompatible and do not induce acute inflammatory responses in the host tissue [46]. Renu et al. reported that  $\text{ZrO}_2$ -NPs cause an increase in GSH and decrease in lipid peroxidation levels [43]. To validate the results of the previous study, the toxicity of  $\text{ZrO}_2$ -NPs was investigated in the present work using antioxidant enzymes (glutathione peroxidase) and non-enzymatic



assays (lipid peroxidation and hematological analysis), apoptosis and necrosis. Our results showed that there was a significant reduction in lipid peroxidation and GSH levels in the tooth gum tissues of diabetic rabbits that had been injected with ZrO<sub>2</sub>-NPs. These findings were consistent with the study by Chakraborty et al., who reported increased lipid peroxidation in the liver and heart in the presence of ZrO<sub>2</sub>-NPs [48]. Several studies examined the reaction of animal cells to ZrO<sub>2</sub>-NPs using MTT assay, wherein cytotoxicity was estimated through evaluation of cell proliferation. The authors reported cytotoxicity associated with ZrO<sub>2</sub>-NPs [49-57]. Results from the present study showed ZrO<sub>2</sub>-NPs decreased succinate dehydrogenase activity and decreased the viability of diabetic rabbit tooth gum cells.

## Conclusion

Within the scope of the present study, it may be concluded ZrO<sub>2</sub>-NPs are not as biocompatible as they were previously assumed. While zirconia may be a compatible biomaterial, reduction of the metal oxide to nano particulates triggers increases in oxidative stress within the mitochondria and disruptions in lysosomal membrane integrity. The cytotoxicity of ZrO<sub>2</sub>-NPs is non-uniform toward body tissues and the most toxic of them is to diabetic rabbit dental tooth gum cells. Accumulation of the NPs in other organs of the diabetic rabbit appears to be minimal. While there is no problem associated with the use of zirconia in bulk, such as in the case of dental implants. Due to the possible concern about the cytotoxicity of zirconia as functional nanoparticles for human dental implants, many specialized investigations should be done in the future.

## Acknowledgments

The results presented in this paper were partly extracted from project of Dr Parvaneh Naserzadeh, assistant professor from Endocrine Research Center, Institute of Endocrinology and Metabolism, Iran University of Medical Sciences, Tehran, Iran, Dr Fatemeh Ghanbary assistant professor from Department of Chemistry, Mahabad Branch, Mahabad, Iran and Dr Seyed Arash Javad Mossavi, researcher from Shahid Beheshti University of Medical Sciences. Tehran, Iran that performed their project under the supervision of Dr Behnaz Ashtari and Dr Parvaneh Naserzadeh. The investigation was carried out in Dr Behnaz Ashtari laboratory at Iran University of Medical Sciences. The authors received no funding from national or international sources.

## Author Contributions

Conceptualization, Parvaneh Naserzadeh, Behnaz Ashtari; Methodology, Parvaneh Naserzadeh; Software, Parvaneh Naserzadeh, Seyed Arash Javad Mossavi; Formal analysis, Parvaneh Naserzadeh, Seyed Arash Javad Mossavi; Investigation, Parvaneh Naserzadeh, Fatemeh Ghanbary, Behnaz Ashtari, Masoud Akhshik; Data curation, Parvaneh Naserzadeh; Writing original draft preparation, Parvaneh Naserzadeh, Behnaz Ashtari;

Writing review and editing, Parvaneh Naserzadeh, Behnaz Ashtari, Masoud Akhshik; Visualization, Parvaneh Naserzadeh, Behnaz Ashtari; supervision, Parvaneh Naserzadeh; project administration, Parvaneh Naserzadeh, Behnaz Ashtari. All authors have read and agreed to the published version of the manuscript.

## Disclosure Statement

The authors declare no conflict of interest.

## References

1. Angélica M, Gomes C, Hauser R, Nunes A, Vitória A (2016) Metal phytoremediation: General strategies, genetically modified plants, and applications in metal nanoparticle contamination. *Ecotoxicol Environ Safety* 134: 133-147.
2. Arora S, Jain J, Rajwade J, Paknikar K (2009) Cellular responses induced by silver nanoparticles: *In vitro* studies. *Toxicol Lett* 179(2): 93-100.
3. Klasson M, Bryngelsson IL, Pettersson C, Husby B, Arvidsson H, et al. (2016) Occupational exposure to cobalt and tungsten in the Swedish hard metal industry: air concentrations of particle mass, number, and surface area. *Ann Occup Hyg* 60(6): 684-99.
4. Minghua L, Suman P, Xue J, Lutz M, Robert D, et al. (2011) Damoiseaux, Stability, Bioavailability, and Bacterial Toxicity of ZnO and Iron-Doped ZnO Nanoparticles in Aquatic Media. *Environ Sci Technol* 45(2): 755-761.
5. Ghosh M, Chakraborty A, Chakraborty A (2013) Cytotoxic, genotoxic and the hemolytic effect of titanium dioxide (TiO<sub>2</sub>) nanoparticles on human erythrocyte and lymphocyte cells *in vitro*. *J Appl Toxicol* 33(10): 1097-1110.
6. Balajia S, Mandala B, Ranjanb S, Dasguptab N, Chidambaramb R (2017) Nano-zirconia-evaluation of its antioxidant and anticancer activity. *J Photochem Photobiol B* 170: 125-133.
7. Misch CE (2004) Dental Implant Prosthetics-E-Book; Elsevier Health Sciences: Amsterdam, The Netherlands.
8. Naujokat H, Kunzendorf B, Wiltfang J (2016) Dental implants and diabetes mellitus, A systematic review. *Int J Implant Dent* 2: 5.
9. Guglielmotti MB, Olmedo DG, Cabrini RL (2019) Research on implants and osseointegration. *Periodontol* 2000 79(1): 178-189.
10. Qasim Al-Fahdawi M, Rasedee A, Sadiq Al-Qubaisi M, Alhassan FH, Rosli R, et al. (2015) Cytotoxicity and physicochemical characterization of iron-manganese-doped sulfated zirconia nanoparticles. *Int J Nanomedicine* 10: 5739-5750.
11. Uusitalo M, Hempel N (2012) Recent advances in intracellular and *in vivo* ROS sensing: focus on nanoparticle and nanotube applications. *Int J Mol Sci* 13: 10660-10679.
12. Singh N, Manshian B, Enkins GJ, Griffiths SM, Williams PM, et al. (2009) Nano Geno toxicology: the DNA damaging potential of engineered nanomaterials. *Biomaterials* 30: 3891-3914.
13. Kubasiewicz P, Dominiak M, Gedrange T, Botzenhart UU (2017) Zirconium: The material of the future in modern implantology. *Adv Clin Experiment Med* 26(3): 533-537.
14. Manicone PF, Iommetti PR, Raffaelli L (2007) An overview of zirconia ceramics: basic properties and clinical applications. *J Dent* 35(11): 819-882.
15. Hingsammer L, Grillenberger M, Schagerl M, Malek M, Hunger S (2018) Biomechanical testing of zirconium dioxide osteosynthesis system for Le Fort I advancement osteotomy fixation. *J Mech Behav Biomed Mater* 77: 34-39.

16. Özkurt Z, Kazazoglu E (2011) Zirconia dental implants: a literature review. *J Oral Implantol* 37(3): 367-376.
17. Nimet D, Adatia D, Stephen C, Lyndon F Cooper, Jeffery Y Thompson (2009) Fracture resistance of yttria-stabilized zirconia dental implant abutments. *J Prosthodont* 18(1): 17-22.
18. Joda T, Voumard B, Zysset P, Brägger U, Ferrari M (2018) Ultimate force and stiffness of 2-piece zirconium dioxide implants with screw-retained monolithic lithium-disilicate reconstructions. *J Prosthodontic Res* 62(2): 258-263.
19. Pirker W, Kocher A (2008) Immediate, non-submerged, root-analogue zirconia implant in single tooth replacement. *Int J Oral Maxillofac Surg* 37(3): 293-295.
20. Abdul L, Muneeb UR, Tahir M, Rehan Khan, Abdul Quaiyoom K, et al. (2013) Farnesol protects against intratracheally instilled cigarette smoke extract-induced histological alterations and oxidative stress in prostate of wistar rats. *Toxicol Int* 20(1): 35-42.
21. Hoffmann O, Angelov N, Gallez F, Jung RE, Weber FE (2008) The zirconia implant-bone interface: a preliminary histologic evaluation in rabbits. *Int J Oral & Maxillofacial Implants* 23(4): 691-695.
22. Salehpour M, Ghanbary F (2016) Synthesis of Cellulose/Zirconium Oxide nanocomposite and the study of its activity in the removal of pollutants. *IIOABJ* 7: 401-408.
23. Bani J, Pugazhendhi A, Venis R (2017) Synthesis and characterization of ZrO<sub>2</sub> nanoparticles-antimicrobial activity and their prospective role in dental care. *Microbial Pathog* 110: 245-251.
24. Díez R, García JJ, Díez MJ, Sierra M, Sahagún AM, et al. (2013) Hypoglycemic and hypolipidemic potential of a high fiber diet in healthy versus diabetic rabbits. *BioMed Res Int* 2013: 1-8.
25. Inaba M (2009) Evaluation of primary stability of inclined orthodontic mini-implants. *J Oral Sci* 51(3): 347-353.
26. Gundersen HJG, Bagger P, Korbo L, Marcussen N, Moller A, et al. (1988) Some new, simple and efficient stereological methods and their use in pathological research and diagnosis. *Apmis* 96(10): 379-394.
27. Kankilic B, Bayramli E, Kilic E, Dağdeviren S, Korkusuz F (2011) Vancomycin containing PLLA/ $\beta$ -TCP controls MRSA *in vitro*. *Clin Orthop Relat Res* 469(11): 3222-3228.
28. Simain Sato F, Lahmouzi J, Heinen E, Defresne MP, De Pauw-Gillet MC, et al. (1999) Graft of autologous fibroblasts in gingival tissue *in vivo* after culture *in vitro* preliminary study on rats. *J Periodontal Res* 34(6): 323-328.
29. Weir A, Westerhoff P, Fabricius L, Goetz N (2012) Titanium dioxide nanoparticles in food and personal care products. *Environ Sci Technol* 46(4): 2242-2250.
30. Duvvuri M, Konkar S, Hong K, Blagg J, Krise P (2006) A new approach for enhancing differential selectivity of drugs to cancer cells. *ACS Chem Biol* 1(5): 309-315.
31. Maleki A, Hosseini MJ, Rahimi N, Abdollahi A, Akbarfakhraei A, et al. (2019) Adjuvant potential of selegiline in treating acute toxicity of aluminium phosphide in rats. *BCPT* 125(1): 62-74.
32. Montazeri S, Bijani S, Anoush M, Sharafi A, Kalantari-Hesari A (2023) Edaravone Improved Behavioral Abnormalities, Alleviated Oxidative Stress Inflammation, and Metabolic Homeostasis Pathways in Depression. *Depression and Anxiety*.
33. Salimi A, Nikoosiar Jahromi M, Pourahmad J (2019) Maternal exposure causes mitochondrial dysfunction in brain, liver, and heart of mouse fetus: An explanation for perfluorooctanoic acid induced abortion and developmental toxicity. *Environ Toxicol* 34(7): 878-885.
34. Soltani M, Hadi Zarei M, Salimi A, Pourahmad J (2019) Mitochondrial protective and antioxidant agents protect toxicity induced by depleted uranium in isolated human lymphocytes. *J Environ Radioact* 203: 112-116.
35. Olson J, Shernoff A, Tarlow J, Colwell JA, Scheetz JP, et al. (2000) Dental osseous implant assessments in a type 2 diabetic population: A prospective study. *Int. J. Oral Maxillofac. Implants* 15(16): 811-818.
36. Oates TW, Galloway P, Alexander P, Vargas Green A, Huynh-Ba G, et al. (2014) The effects of elevated hemoglobinA(1c) in patients with type 2 diabetes mellitus on dental implants: Survival and stability at one year. *J Am Dent Assoc* 145(12): 1218-1226.
37. Sharma S, Bano S, Ghosh AS, Mandal M, Hae-Won K, et al. (2016) Silk fibroin nanoparticles support *in vitro* sustained antibiotic release and osteogenesis on titanium surface, *Nanomedicine: Nanomedicine* 12(5): 1193-1204.
38. Simon HU, Haj-Yehia A, Levi-Schaffer F (2000) Role of reactive oxygen species (ROS) in apoptosis induction, *Apoptosis*, 5(5): 415-418.
39. Wang F, Jiao C, JLiuc J, Yuana H, Lan M, Gao F (2011) Oxidative mechanisms contribute to nanosize silican dioxide-induced developmental neurotoxicity in PC12 cells, *Toxicology in Vitro* 25(8): 1548-1556.
40. Wu J, Sun J, Xue Y (2010) Involvement of JNK and P53 activation in G2/M cell cycle arrest and apoptosis induced by titanium dioxide nanoparticles in neuron cells. *Toxicol Lett* 199(3): 269-276.
41. Asadpour E, Sadeghnia H, Ghorbani A, Sedaghat M, Boroushaki M (2016) Oxidative stress-mediated cytotoxicity of zirconia nanoparticles on PC12 and N2<sub>a</sub> cells. *J Nanoparticle Res* 18-14.
42. Asadpour E, Sadeghnia H, Ghorbani A, Taher Boroushaki M (2014) Effect of zirconium dioxide nanoparticles on glutathione peroxidase enzyme in PC12 and N2<sub>a</sub> cell lines. *Iran J Pharm Res* 13(4): 1141-1148.
43. Blair Ian A (2008) DNA adducts with lipid peroxidation products. *J Biol Chem* 283(23): 15545-15549.
44. Khodaghali F, Ansari N, Amini M, Khoramian Tusi S (2012) Involvement of molecular chaperones and the transcription factor Nrf<sub>2</sub> in neuroprotection mediated by para-substituted-4, 5-diaryl-3-thiomethyl-1, 2, 4-triazines. *Cell Stress Chaperones* 17(4): 409-422.
45. Hanley C, Thurber A, Hanna C, Punnoose A, Zhang J, et al. (2009) The influences of cell type and ZnO nanoparticle size on immune cell cytotoxicity and cytokine induction, *Nanoscale research letters* 4(12): 1409.
46. Vairapandi M (2003) Characterization of DNA demethylation in normal and cancerous cell lines and the regulatory role of cell cycle proteins in human DNA demethylase activity. *J Cell Biochem* 91(3): 572-583.
47. Ruichan, Yang G, He F, Yunlu Dai, Gai S, et al. (2013) Mesoporous NaYF<sub>4</sub>: Yb, Er@Au-Pt (IV)-FA nanospheres for dual-modal imaging and synergistic photothermal/chemo- anti-cancer therapy, *RSC Advances* 1-3.
48. Rani V, Deep G, Singh KR, Palle K, Yadave S (2016) Oxidative stress and metabolic disorders: Pathogenesis and therapeutic strategies. *Life Sci* 148: 183-193.
49. Renu Kowluru A, Mishra M (2017) Epigenetic Regulation of Redox Signaling in Diabetic Retinopathy: Role of Nrf<sub>2</sub>, *Free Radic Biol Med* 103: 155-164.
50. Tammina S, Mandal B, Ranjan S, Dasgupta N (2017) Cytotoxicity study of Piper nigrum seed mediated synthesized SnO<sub>2</sub> nanoparticles towards colorectal (HCT116) and lung cancer (A549) cell lines. *J Photochem Photobiol B* 166: 158-168.

51. Caicedo M, Jacobs J, Reddy A, Halla N (2018) Analysis of metal ion-induced DNA damage, apoptosis, and necrosis in human (Jurkat) T-cells demonstrates Ni<sup>2+</sup> and V<sup>3+</sup> are more toxic than other metals: Al<sup>3+</sup>, Be<sup>2+</sup>, Co<sup>2+</sup>, Cr<sup>3+</sup>, Cu<sup>2+</sup>, Fe<sup>3+</sup>, Mo<sup>5+</sup>, Nb<sup>5+</sup>, Zr<sup>2+</sup>. J Biomed Mater Res A 86(4): 905-913.
52. Damestani Y, Hoffman E, Ortiz D, Cabrales P, Aguilar G (2016) Inflammatory response to implantation of transparent nanocrystalline yttria-stabilized zirconia using a dorsal window chamber model. Nanomedicine 12(7): 1757-1763.
53. Renu Kowluru A, Mishra M (2017) Epigenetic Regulation of Redox Signaling in Diabetic Retinopathy: Role of Nrf<sub>2</sub>. Free Radic Biol Med 103: 155-164.
54. Chakraborty S, Mahapatra S, Sahu S, Pramanik P, Roy S (2011) Antioxidative effect of folate-modified chitosan nanoparticles, Asian Pac J Trop Biomed 1(1): 29-38.
55. Shukla S, Jadaun A, Arora V, Sinha RK, Biyani N, et al. (2014) *In vitro* toxicity assessment of chitosan oligosaccharide coated iron oxide nanoparticles. Toxicol Rep 2: 27-39.
56. Kilic K, Kesim B, Sumer Z, Polat Z, Kesim S (2013) *In vitro* cytotoxicity of all-ceramic substructural materials after aging. J Dent Sci 8(3): 231-238.
57. Sjögren G, Sletten G, Dahl JE (2000) Cytotoxicity of dental alloys, metals, and ceramics assessed by millipore filter, agar overlay, and MTT tests. J Prosthet Dent 84(2): 229-236.



This work is licensed under Creative Commons Attribution 4.0 License  
DOI: [10.19080/OAJT.2023.05.555673](https://doi.org/10.19080/OAJT.2023.05.555673)

## Your next submission with Juniper Publishers will reach you the below assets

- Quality Editorial service
- Swift Peer Review
- Reprints availability
- E-prints Service
- Manuscript Podcast for convenient understanding
- Global attainment for your research
- Manuscript accessibility in different formats  
( Pdf, E-pub, Full Text, Audio)
- Unceasing customer service

Track the below URL for one-step submission  
<https://juniperpublishers.com/online-submission.php>